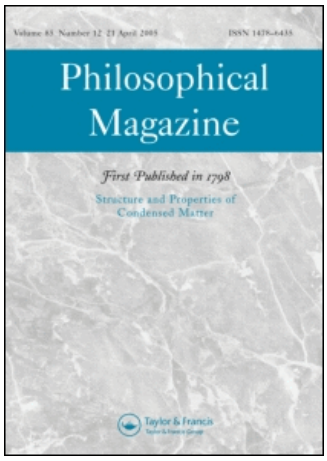

Philosophical Magazine
First published in 1798
Publication details, including instructions for authors and subscription information:
http://www.informaworld.com/smpp/title~content=t713695589

Structured diffuse scattering, local crystal chemistry and metal ion ordering in the (1 - **x**)MgS · $^{\mathbf{x}}/_{3}Yb_2S_3$, 0 ≤ **x**≤ ? 0.45, 'defect' NaCl system

Online Publication Date: 01 July 2007
To cite this Article: Withers, R. L., Urones-Garrote, E. and Otero-Diaz, L. C. , (2007) 'Structured diffuse scattering, local crystal chemistry and metal ion ordering in the (1 - **x**)MgS · $^{\mathbf{x}}/_{3}Yb_2S_3$, 0 ≤ **x**≤ ? 0.45, 'defect' NaCl system', Philosophical Magazine, 87:18, 2807 - 2813
To link to this article: DOI: 10.1080/14786430601078017
URL: http://dx.doi.org/10.1080/14786430601078017

Philosophical Magazine,
Vol. 87, Nos. 18–21, 21 June–21 July 2007, 2807–2813

Structured diffuse scattering, local crystal chemistry and metal ion ordering in the $(1-x)MgS \cdot {}^{x}/_{3}Yb_2S_3$, $0 \leq x \leq \sim 0.45$, 'defect' NaCl system

R. L. WITHERS*†, E. URONES-GARROTE‡ and L. C. OTERO-DIAZ‡

†Research School of Chemistry, Australian National University, Canberra, ACT, 0200, Australia
‡Facultad de Ciencias Químicas, Dipartamento di Química Inorgánica, Universidad Complutense, E-28040, Madrid, Spain

(*Received 23 September 2006; in final form 12 October 2006*)

Rare earth sulfide solid solutions of 'defect' NaCl average structure type exhibit excellent colour characteristics and thus represent good prospects for use in the paints and plastics industry. As the colour characteristics of such systems are closely related to the local distribution of rare earth ions, it is important to know as much as possible about the latter. In this contribution, the reciprocal space shape of a highly structured, diffuse intensity distribution observed in a $(1-x)MgS \cdot xYb_{2/3}S$, $x = 0.30$, sample is used to show that the smallest polyhedral building blocks of the average NaCl structure type should each have, as far as possible, the same composition as the overall macroscopic composition. Local crystal chemical considerations suggest that both the Yb^{3+} ions and the vacancies $\square$ would prefer to be opposite Mg^{2+} ions.

1. Introduction

Growing environmental restrictions, as a result of the toxicity of 'traditional' inorganic pigments [1], such as Cd(S, Se), mean that there is an ever-increasing need for new environmentally acceptable pigments. Rare earth sulfide solid solutions, e.g. $(1-x)MgS \cdot xYb_{2/3}S = Mg_{1-x}Yb_{2x/3}\square_{x/3}S$, $0 \leq x \leq 0.45$ and $\square$ a vacancy, of 'defect' NaCl average structure type, exhibit excellent colour characteristics and, thus, have good prospects for use in the paints and plastics industry [2–4]. The existence of wide range, non-stoichiometric $(1-x)M^{2+}S \cdot xLn^{3+}_{2/3}S$, $M^{2+} = Mg$, Mn, Ca, $Ln^{3+} =$ rare earth element or Y, solid solutions of this type with average 'defect' NaCl structure type has long been known [5–7]. The arrangement of the metal ions on the local scale, however, has not. As the colour characteristics of such systems are

*Corresponding author. Email: withers@rsc.anu.edu.au

Philosophical Magazine
ISSN 1478–6435 print/ISSN 1478–6443 online © 2007 Taylor & Francis
http://www.tandf.co.uk/journals
DOI: 10.1080/14786430601078017

closely related to the local distribution of rare earth ions, it is important to know as much as possible about the latter.

2. Experimental

2.1. *Synthesis*

Samples with nominal composition $(Mg_{1-x}Yb_{2x/3}\square_{x/3})S$, $0 < x \leq 0.45$, were grown following the synthetic procedures outlined in [2].

2.1.1. X-ray diffraction. X-ray powder diffraction (XRD) patterns were collected using a Philips X'pert Diffractometer with Cu $K_{\alpha 1}$ radiation. Silicon (NBS No. 640) was used as an internal standard to accurately determine unit cell parameters.

2.1.2. Electron microscopy. Transmission Electron Microscope (TEM) analysis was carried out on Philips EM 430 and CM 200 FEG TEM's as well as on a JEOL JEM 3000 F TEM, on crushed grains of the samples dispersed onto holey carbon-coated copper grids.

3. Results and discussion

3.1. *X-ray diffraction*

Up to $x = 0.30$, the samples appeared single phase with an average rocksalt or NaCl type structure. For $x > 0.45$, the dominant phase was of spinel type while a two phase region occurs in between according to XRPD. For $x \leq 0.3$, the lattice parameter of the 'defect NaCl' average structure systematically expands from $a = 5.188(4)$ Å for the end-member MgS composition to 5.282(4) Å for $x = 0.30$. For the purposes of maximizing the visibility of the diffuse distribution, the sample with the greatest concentration of Yb^{3+} ions which is apparently still in the single phase 'defect NaCl' solid solution field, i.e. $x = 0.30$, was used for investigation in the electron microscope.

3.2. *Electron microscopy*

Figure 1 shows typical (a) ⟨001⟩, (b) ⟨201⟩, (c) ⟨301⟩, (d) ⟨110⟩, (e) ⟨114⟩ and (f) ⟨111⟩ zone axis electron diffraction patterns (EDP's) typical of the $x = 0.30$ 'defect NaCl' solid solution.

In addition to the strong Bragg reflections of the underlying *Fm*-3m, 'defect NaCl', average structure, note the presence of a spectacular, highly structured, characteristic diffuse intensity distribution, as well as the occasional presence of what appear to be $\mathbf{G} \pm 1/n$ ⟨111⟩*, n an integer, satellite reflections, e.g. the

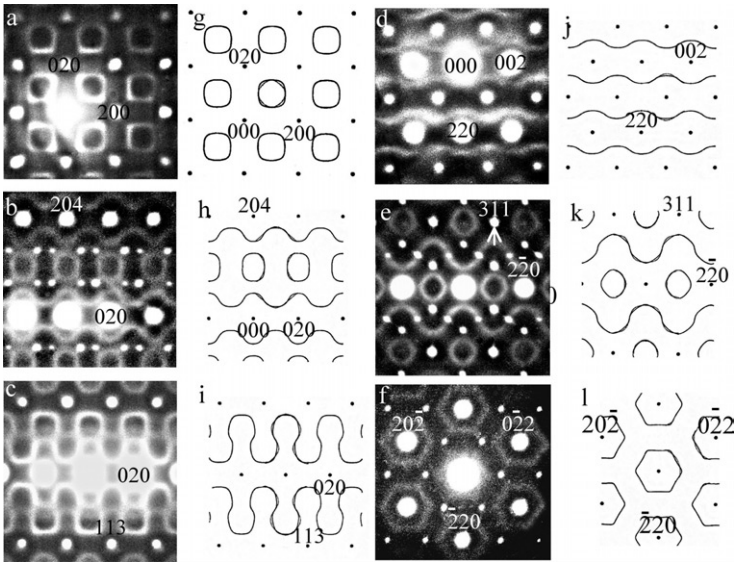

Figure 1. (a) ⟨001⟩, (b) ⟨201⟩, (c) ⟨301⟩, (d) ⟨110⟩, (e) ⟨114⟩ and (f) ⟨111⟩ zone axis EDPs of the $x = 0.30$ 'defect NaCl' solid solution. (g)–(l) Equivalent calculated sections through the diffuse surface $\cos \pi h + \cos \pi k + \cos \pi l = 0$ (taken from [8]).

$\mathbf{G} \pm 1/3$ ⟨224⟩* $\equiv \mathbf{G}' \pm 1/3$ ⟨−1, −1, 1⟩* reflections in figure 1b or the $\mathbf{G} \pm 1/3$ ⟨5, −1,1⟩* $\equiv \mathbf{G}' \pm 1/3$ ⟨−1, −1, 1⟩* reflections in figure 1e. The reason for the apparent existence of the latter $\mathbf{G} \pm 1/n$ ⟨111⟩* diffuse streaking is the existence, in some regions of the sample, of very thin {111} planar defects giving rise to continuous diffuse streaking along the $\mathbf{G} \pm \gamma$ ⟨111⟩*, γ continuous, directions of reciprocal space (see figure 2). The planar precipitates have previously been shown to be of spinel type (see [2]). Given that these planar precipitates are usually fairly widely spaced, however, they should affect the stoichiometry of the remaining 'defect NaCl' solid solution to only a very small extent. We have therefore ignored their presence in the following analysis of the 'defect NaCl' solid solution.

Turning now to the observed highly structured diffuse distribution, the similarity of the calculated sections shown in figure 1g through figure 1l (taken from the much earlier work of Sauvage and Parthé [8] on vacancy ordering in sub-stoichiometric transition metal carbides and nitrides) with the corresponding experimental EDP's shown in figure 1a through figure 1f leaves no doubt that the diffuse intensity surface describing the observed diffuse distribution can be described to a quite good zeroth order approximation by the equation $\cos \pi h + \cos \pi k + \cos \pi l = 0$, where $\mathbf{q} = h\mathbf{a}^* + k\mathbf{b}^* + l\mathbf{c}^*$ and h, k and l are here understood to be continuous reciprocal space variables. As shown in [8–10], such an equation is the result of a strongly obeyed nearest neighbour six-body constraint, in this case a requirement that the composition of the nearest neighbour (nn) octahedral cluster surrounding each S ion (see figure 3) should each have a stoichiometry as close as possible to the overall macroscopic stoichiometry.

In the language of modulated structures, where the deviation of the local stoichiometry of the metal ion site at $(\mathbf{t} + \mathbf{r}_M)$, $\mathbf{t}$ a Bravais lattice vector and $\mathbf{r}_M$ the

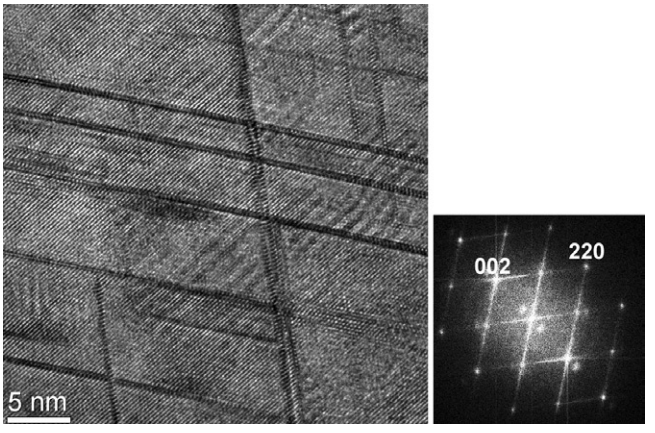

Figure 2. (a) ⟨110⟩ HREM lattice image showing thin {111} planar defects of spinel type [2] intergrown in the 'defect NaCl' average structure type. (b) The direct Fourier transform of this HREM image.

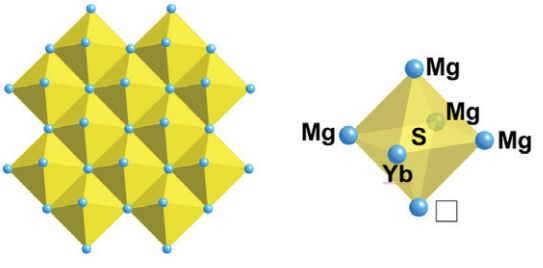

Figure 3. Shows the defect NaCl average structure type in projection close to ⟨001⟩ (the constituent SM_6 octahedra are shown in yellow) along with the most common $S(Mg_4Yb_1\square_1)$ octahedral cluster surrounding any one particular S ion.

position of the metal ion in the parent unit cell, from the average, can be written in the form $\delta f_M(\mathbf{t}+\mathbf{r}_M) = f_M^{av} a_M(\mathbf{q}) \exp 2\pi i\mathbf{q}.(\mathbf{t}+\mathbf{r}_M)$ [10, 11], we thus require

$$\begin{aligned}
&\delta f_M\left(\mathbf{t}+\frac{1}{2}\mathbf{a}\right)+\delta f_M\left(\mathbf{t}-\frac{1}{2}\mathbf{a}\right)+\delta f_M\left(\mathbf{t}+\frac{1}{2}\mathbf{b}\right)+\delta f_M\left(\mathbf{t}-\frac{1}{2}\mathbf{b}\right)\\
&\quad+\delta f_M\left(\mathbf{t}+\frac{1}{2}\mathbf{c}\right)+\delta f_M\left(\mathbf{t}-\frac{1}{2}\mathbf{c}\right)\\
&=2f_M^{av}\sum\nolimits_q a_M(\mathbf{q})\exp 2\pi i\mathbf{q}.\mathbf{t}\left\{\cos 2\pi\mathbf{q}.\frac{1}{2}\mathbf{a}+\cos 2\pi\mathbf{q}.\frac{1}{2}\mathbf{b}+\cos 2\pi\mathbf{q}.\frac{1}{2}\mathbf{c}\right\}\\
&=0 \text{ for all } \mathbf{t}
\end{aligned}$$

This needs to be true not just for the S ion at **t** but for all the S ions whatever the value of **t**. The only values of **q** which can satisfy this requirement are therefore those

for which $\{\cdots\} = \cos\pi h + \cos\pi k + \cos\pi l = 0$, as observed to a very good approximation (see figure 1).

Given an average structure stoichiometry for $x = 0.30$ of $Mg_{0.7}Yb_{0.2}\square_{0.1}S$, this amounts to a requirement that each S ion should always be surrounded, as far as possible, by the average number of metal ions, i.e. 4.2 Mg's, 1.2 Yb's and 0.6 vacancies for $x = 0.30$. In turn, this implies the most common local octahedral configurations surrounding any particular S ion must be $Mg_4Yb_1\square_1$ (as shown in figure 3), $Mg_5Yb_1\square_0$ and $Mg_4Yb_2\square_0$. The overall stoichiometry results if only these three local configurations occur and if the relative proportions of their occurrence are 60%, 20% and 20%, respectively.

Note that the above six body nn constraint says nothing about the relative arrangement of the constituent metal ions around the S ions or of the relative orientation of the local configurations. Local crystal chemical considerations, however, suggest that such constraints must exist. Table 1, for example, shows the calculated bond valence sums, or Apparent Valences (AVs) [12], of the various constituent ions depending upon their local co-ordination environment and assuming (at this stage) no local structural relaxation accompanying the compositional metal ion ordering. It can be seen that the Mg^{2+} ions, under these conditions, are under-bonded by ~13.7% and hence, will seek to attract neighbouring S ions while the Yb^{3+} ions are over-bonded by ~13.1% and hence will seek to repel neighbouring S ions (the ideal $M-S^{2-}$ separation distance for octahedral co-ordination is given by $R_{ideal}(Mg^{2+}-S^{2-}) = 2.587$ Å in the case of $M = Mg^{2+}$ and $R_{ideal}(Yb^{3+}-S^{2-}) = 2.687$ Å in the case of $M = Yb^{3+}$. Keep in mind that the average $M-S^{2-}$ separation distance is given by $a/2 = 2.641$ Å for $x = 0.30$). From the point of view of minimizing local strain, it would, therefore, make crystal chemical commonsense for an Yb^{3+} ion to always be opposite a Mg^{2+} ion. Likewise a $\square$ will repel a S^{2-} ion and, therefore, from the point of view of strain minimization, should again always be opposite a Mg^{2+} ion (as shown in figure 3).

The above crystal chemical considerations suggest the need for an additional longer range constraint on the pattern of metal ion ordering surrounding each S ion. The next nn polyhedron of metal ions surrounding each S ion is a cubic cluster at $\mathbf{t} \pm {}^{1}/_{2}\langle 111\rangle$, as shown in figure 4. Applying the same requirement as that used above to this cluster, i.e. its composition or stoichiometry should be as

Table 1. Calculated bond valence sums or AV's of the various constituent ions depending upon their local co-ordination environment. No structural relaxation away from the average structure has been allowed.

Atom	AV	Ideal AV
Mg	1.726	2.0
Yb	3.392	3.0
$S(Mg_4Yb_1\square_1)$	1.716	2.0
$S(Mg_4Yb_2\square_0)$	2.281	2.0
$S(Mg_5Yb_1\square_0)$	2.004	2.0

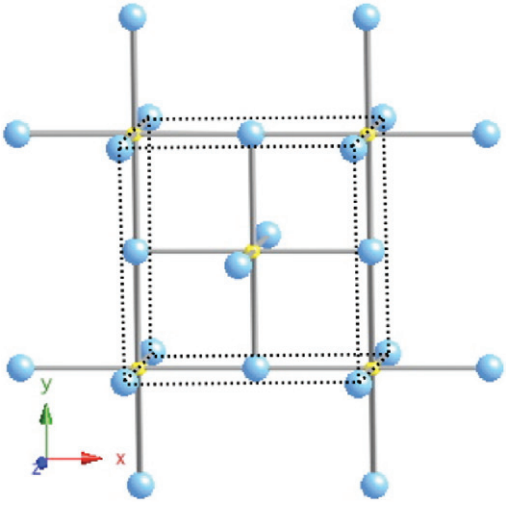

Figure 4. Shows the next nn SM_8 cubic cluster of metal ions (dashed lines) surrounding each S ion at $\mathbf{t} \pm 1/2\ \langle 111 \rangle$.

close as possible to the overall stoichiometry of $Mg_{5.6}Yb_{1.6}\square_{0.8}$, gives rise to the constraint equation

$$\begin{aligned}
&..\delta f\mathrm{M}\left(\mathbf{t}+\frac{1}{2}[111]\right)+\delta f\mathrm{M}\left(\mathbf{t}-\frac{1}{2}[111]\right)+\delta f\mathrm{M}\left(\mathbf{t}+\frac{1}{2}[-1,-1,-1]\right)\\
&\quad+\delta f\mathrm{M}\left(\mathbf{t}-\frac{1}{2}[-1,-1,1]\right)+\delta f\mathrm{M}\left(\mathbf{t}+\frac{1}{2}[1,-1,-1]\right)\\
&\quad+\delta f\mathrm{M}\left(\mathbf{t}-\frac{1}{2}[1,-1,-1]\right)+\delta f\mathrm{M}\left(\mathbf{t}+\frac{1}{2}[-1,1,-1]\right)+\delta f\mathrm{M}\left(\mathbf{t}-\frac{1}{2}[-1,1,-1]\right)\cdots\\
&=2f_{\mathrm{M}}^{av}\sum_{q}a_{\mathrm{M}}(\mathbf{q})\exp 2\pi i\mathbf{q}.\mathbf{t}\,\{4\cos\pi h.\cos\pi k.\cos\pi l\}\cdots=0 \text{ for all } \mathbf{t}.
\end{aligned}$$

The only values of $\mathbf{q}$ which can satisfy this requirement are those for which $\{\cdots\}=4\cos\pi h.\cos\pi k.\cos\pi l=0$. Of course, both the $\cos\pi h+\cos\pi k+\cos\pi l=0$ and $4\cos\pi h.\cos\pi k.\cos\pi l=0$ constraints cannot be simultaneously satisfied, so that it is necessary to weight the two constraints as follows:

$$\{\cos\pi h+\cos\pi k+\cos\pi l\}-\gamma\{4\cos\pi h.\cos\pi k.\cos\pi l\}\cdots=0.$$

The parameter γ in the above constraint equation defines the relative weight given to the separate constraints. Experimentally, by fitting to the experimental EDPs shown in figure 1, γ is estimated to be $\sim$2.6(6). In the case of the sub-stoichiometric transition metal carbides and nitrides, which give structured diffuse distributions rather similar to those reported here [8], γ was found to range experimentally between 0 and 0.75. The effect of adding this second nn constraint to the first nn constraint is to square up somewhat the experimentally observed diffuse distribution, as can be qualitatively understood from a comparison of the shape of the individual

$\cos \pi h + \cos \pi k + \cos \pi l = 0$ and $4\cos \pi h.\cos \pi k.\cos \pi l = 0$ diffuse distributions (cf., for example, figure 3a with figure 3b of [9]).

Clearly, there are very strong local crystal chemical rules as regards the distribution of the M^{2+}, Ln^{3+} and $\square$ ions on the metal ion sites of the average defect NaCl structure type of these rare earth solid solution phases. Direct information as to these real space local ordering rules is readily available in the form of the detailed shape of the corresponding diffuse intensity distributions in reciprocal space.

References

[1] J.N. Berte, in *High Performance Pigments*, edited by H.M. Smith (Wiley–VCH, Weinheim, 2002), pp. 27–50.
[2] E. Urones-Garrote, A. Goméz-Herrero, A.R. Landa-Canovas, *et al*., J. Alloys Compd. **374** 197 (2004).
[3] E. Urones-Garrote, A. Goméz-Herrero, A.R. Landa-Canovas, *et al*., Chem. Mater. **17** 3524 (2005).
[4] M.D. Hernández-Alonso, A. Gómez-Herrero, A.R. Landa-Cánovas, *et al*., J. Alloys Compd. **323/324** 297 (2001).
[5] J. Flahaut, in *Handbook on the Physics and Chemistry of the Rare Earths*, edited by K.L. Gschneider and L. Eyring, Chapter 31, Vol. 4 (North Holland, Amsterdam, 1979), pp. 1–88.
[6] J.K. Burdett and J.F. Mitchell, Prog. Solid State Chem. **23** 131 (1995).
[7] M. Patrie, J. Flahaut and L. Domange, Rev. Hautes Temp. Réfract. **2** 18 (1965).
[8] M. Sauvage and E. Parthé, Acta Crystallogr. A **28** 607 (1972).
[9] R. de Ridder, G. van Tendeloo and S. Amelinckx, Acta Crystallogr. A **32** 216 (1976).
[10] R.L. Withers, S. Schmid, L. Norén, *et al*., Ferroelectrics **250** 47 (2001).
[11] R.L. Withers, S. Schmid and J.G. Thompson, Prog. Solid State Chem. **26** 1 (1998).
[12] N.E. Brese and M. O'Keeffe, Acta Crystallogr. B **47** 192 (1991).